Journal of Hydrology: Regional Studies 6 (2016) 52–65

Contents lists available at ScienceDirect

Journal of Hydrology: Regional Studies

journal homepage: www.elsevier.com/locate/ejrh

Spatial and temporal characteristics of precipitation over the Three-River Headwaters region during 1961–2014

Haiyun Shi[a,b,c,*], Tiejian Li[a,c], Jiahua Wei[a,c], Wang Fu[a], Guangqian Wang[a,c]

[a] State Key Laboratory of Hydroscience and Engineering, Tsinghua University, Beijing, China
[b] Department of Civil Engineering, The University of Hong Kong, Hong Kong, China
[c] School of Water Resources and Electric Power, Qinghai University, Xining, Qinghai, China

ARTICLE INFO

Article history:
Received 2 September 2015
Received in revised form 15 March 2016
Accepted 20 March 2016
Available online 30 March 2016

Keywords:
Precipitation
Temporal trend
Spatial distribution
Elevation
Runoff
Three-River Headwaters region

ABSTRACT

Study region: Three-River Headwaters (TRH) region, China.
Study focus: Precipitation is regarded as the basic component of the global hydrological cycle. This study investigated the spatial and temporal characteristics of precipitation over the TRH region during 1961–2014, based on the observed data of 29 meteorological stations.
New hydrological insights for the region: The results showed that: (1) temporally, the TRH region has experienced a significant increasing trend in the annual precipitation ($p < 0.1$) during 1961–2014, especially in the dry season ($p < 0.01$). (2) Spatially, the mean annual precipitation (MAP) in the TRH region showed the southeast-to-northwest decreasing trend and the annual precipitation recorded at most stations (i.e., 26 in 29) presented the increasing trends. (3) A close correlation of the MAP with elevation was found, that is, a low-to-high increasing trend below 3800 m but an inverse correlation above 3800 m; in addition, statistical equations to estimate precipitation with high R^2 values were established based on longitude, latitude and elevation. (4) Characteristics of related meteorological variables and possible impact of precipitation on runoff were analyzed and discussed. These results would be valuable for the researchers to better understand the changing characteristics of precipitation and for the managers to make better decisions in the future.

1. Introduction

As a basic meteorological variable, precipitation is an excellent indicator widely used in the fields of integrated water resources management, crop water requirements prediction, and ecological environment assessment. In the past century, global climate change (e.g., the significant increase in air temperature), which has greatly influenced the water circulation and hydrological processes (Garbrecht et al., 2004; Novotny and Stefan, 2007; IPCC, 2007), has drawn the attention of numerous researchers. In most regions, climate change indeed caused dramatic changes in precipitation (Liu et al., 2008; Chen and Chu, 2014; Zarch et al., 2015); however, the changing characteristics was quite different among regions. Several studies have indicated that precipitation generally presented an increasing trend in the Northern Hemisphere in the past several decades (Groisman et al., 2005; IPCC, 2007; Westra et al., 2013; Cao and Pan, 2014; Fan et al., 2014). The same trend has been found in most regions of China, including the western China, the Yangtze River basin, and the southeastern coast;

* Corresponding author at: State Key Laboratory of Hydroscience and Engineering, Tsinghua University, Beijing, China.
E-mail addresses: shihaiyun@tsinghua.edu.cn (H. Shi), litiejian@tsinghua.edu.cn (T. Li), weijiahua@tsinghua.edu.cn (J. Wei), fuw14@mails.tsinghua.edu.cn (W. Fu), dhhwgq@tsinghua.edu.cn (G. Wang).

http://dx.doi.org/10.1016/j.ejrh.2016.03.001
2214-5818/

however, precipitation has shown a decreasing trend over the north China and the Sichuan Basin (Zhai et al., 2005). Thus, it is necessary to investigate the spatial and temporal characteristics of precipitation for the designated region.

Specifically, the Three-River Headwaters (noted as TRH hereafter) region, a plateau mountainous region in the western China, is particularly sensitive to climate change, which may bring serious disturbances to the ecosystem (Fan et al., 2010; Immerzeel et al., 2010; Zhang et al., 2013; Tong et al., 2014; Zhu et al., 2015). With reference to precipitation, Liang et al. (2013) reported an increasing trend in the annual precipitation across the TRH region during 1960–2009 using the observed data from 12 meteorological stations. Yi et al. (2013) reached a similar finding through analyzing the monthly data during 1961–2010; however, the seasonal precipitation presented the decreasing trends during the same period in some parts of the TRH region. Based on the observed data from 43 meteorological stations inside or around the TRH region, Tong et al. (2014) indicated that the annual precipitation generally showed an increasing trend from 1990 to 2012, and such trend was more obvious with significant fluctuations after 2004. Moreover, changes in precipitation extremes were investigated by using the daily data from 12 meteorological stations, and the results demonstrated that most of the selected indices exhibited the increasing trends during 1960–2012 (Cao and Pan, 2014).

It is worth noting that precipitation can be characterized by significant spatial variation for regions with large elevation variations (e.g., the TRH region in this study). Normally, the relationship between precipitation and elevation can be expressed by various functional forms, such as linear, logarithmic and exponential (e.g., Osborn, 1984; Daly et al., 1994; Naoum and Tsanis, 2004; Shi, 2013). Overall, the studies of the relationship between these two variables indicated that the dominant impact factor is the local climate. For example, precipitation may generally increase along with the increase of elevation in most regions, (e.g., Goovaerts, 2000; Chu, 2012); however, above a certain altitude, precipitation may decrease with elevation increase (e.g., Schermerhorn, 1967). Therefore, it is valuable to explore the relationship between precipitation and elevation. Moreover, precipitation can be influenced by a variety of related meteorological variables, such as air pressure, air temperature, wind speed, and so on (Singh, 1988; Benestad, 2013; Makarieva et al., 2014). In the past several decades, air temperature in the TRH region has presented a significant increasing trend (Liang et al., 2013), along with the global warming; and wind speed has been reducing worldwide (e.g., McVicar et al., 2008; Pryor et al., 2009). These meteorological variables may have great effects on the spatial and temporal characteristics of precipitation in the TRH region, which should be further studied.

The objective of this study is to investigate the temporal trend and spatial distribution of precipitation over the TRH region during 1961–2014. The daily precipitation data recorded at 29 meteorological stations are used in this study. Compared to previous studies (e.g., Liang et al., 2013; Yi et al., 2013; Cao and Pan, 2014), the significance of this study can be described as follows: first, 17 more meteorological stations are used to obtain more reliable results of the spatiotemporal patterns of precipitation. Second, this study aims to establish statistical equations to estimate precipitation based on longitude, latitude and elevation, which would be useful to understand the local climate. Third, the changing characteristics of related meteorological variables are analyzed, and the mechanism of the impacts of these meteorological variables on precipitation is discussed. Fourth, possible impact of precipitation on runoff is also quantitatively analyzed in different river basins through calculating the change of runoff from the changed precipitation, which may either mitigate the decreasing trend in runoff or contribute to the increasing trend in runoff. This would be helpful to provide a scientific basis for the changing characteristics of precipitation in such regions.

2. Data and methodology

2.1. Study area and research data

The TRH region, which is well-known as the sources of the Yangtze River, the Yellow River and the Lantsang River, is located in the Qinghai Province in the western China (89°45′-102°23′ E, 31°39′-36°12′ N) (see Fig. 1). With an area of 0.3 million km^2, it accounts for 43% of the total area of the Qinghai Province (Cao and Pan, 2014). The elevation of this region varies between 2000 m and 6600 m, and the mean value is over 4000 m. This region lies in the temperate zone, mainly dominated by a plateau monsoon climate. Normally, the annual precipitation ranges from 262 mm to 773 mm in this region (Yi et al., 2013), and more than 80% of the annual precipitation occurs in the wet season from May to October (Liang et al., 2013).

There are 37 meteorological stations available inside or around the study area (see Table 1 for details). The daily observed data can be downloaded for free on the official website of China Meteorological Administration (China Meteorological Administration, 2016). As most of these stations were built in the late 1950s, only the data from 1961 are selected in this study to ensure that the lengths of the datasets from different stations are consistent. For the designated station, missing data are interpolated using the data of the neighboring stations in the same years; however, stations with serious lack of data (i.e., more than twenty years) are excluded directly. After this elimination, there are 29 meteorological stations left with complete daily observations from 1961 to 2014. The annual and seasonal precipitation can be derived from the daily values. In order to test the general trend of precipitation over the TRH region, the Thiessen polygon method (Thiessen and Alter, 1911; Brassel and Reif, 1979) is adopted to interpolate the precipitation data from different stations to obtain the mean annual and seasonal precipitation values. Yearly anomalies are achieved by removing the long-term means. Moreover, related meteorological data (e.g., air pressure, air temperature, relative humidity, and wind speed) are also used to analyze their relationships with precipitation.

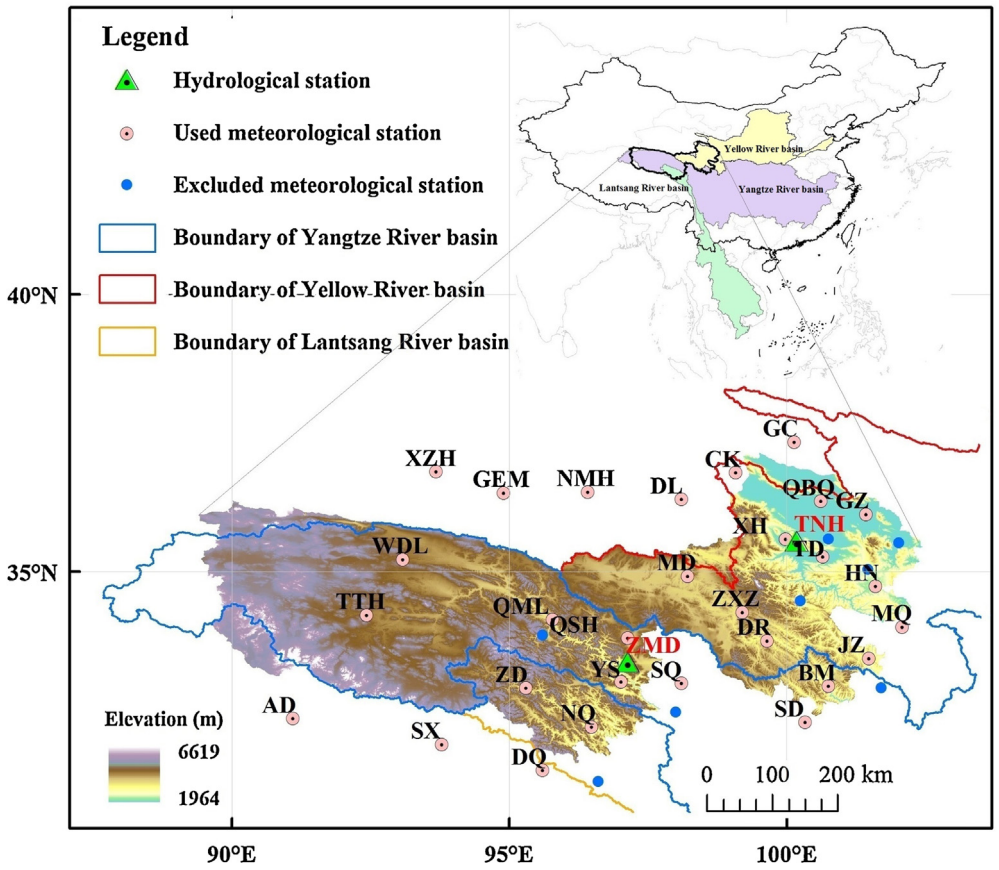

Fig 1. The locations of meteorological and hydrological stations in the TRH region.

In addition, the annual runoff data recorded at two hydrological stations are used to investigate the relationship between runoff and precipitation in this region, namely, the Tangnaihai (TNH) station and the Zhimenda (ZMD) station. The TNH station (100°10′ E, 35°33′ N, with the drainage area of 121,972 km^2) is an important control station in the upper Yellow River, while the ZMD station (97°07′ E, 33°22′ N, with the drainage area of 137,704 km^2) is the key station in the upper Yangtze River (Fig. 1). The data recorded at these two stations are both available from 1956 to 2013, which were provided by the Hydrology and Water Resources Bureau of Qinghai Province, China.

2.2. Trend test and change point test methods

The temporal variations of precipitation and related meteorological data are analyzed by using the trend test and change point test methods, as shown in the following.

1) Trend test method

Mann-Kendall trend test is a nonparametric rank-based statistical test that was first proposed by Mann (1945) and further developed by Kendall (1975), and it is widely used in the fields of meteorology, hydrology and sedimentology (Changnon and Demissie, 1996; Burn and Elnur, 2002; Novotny and Stefan, 2007; Jones et al., 2015; Shi and Wang, 2015; Zhang et al., 2015).

Based on the Mann-Kendall trend test method, the slope of the series can be computed by using the Thiel-Sen method (Thiel, 1950; Sen, 1968).

$$\beta = Median\left(\frac{X_j - X_i}{j - i}\right), \text{ for all } i < j \tag{1}$$

where X_j and X_i are the observed values in the j-th and i-th year ($j > i$), respectively.

Table 1
General information of the meteorological stations in the TRH region.

Station name	Abbreviation	Longitude (°E)	Latitude(°N)	Elevation(m)	Years with observed data
Xiaozhaohuo	XZH	93.68	36.80	2767	1960–2009
Gangcha	GC	100.13	37.33	3321	1957–2009
Geermu	GEM	94.9	36.42	2807.6	1955–2009
Nuomuhong	NMH	96.42	36.43	2790	1956–2009
Dulan	DL	98.10	36.30	3191	1954–2009
Chaka	CK	99.08	36.78	3088	1955–2000
Qiaboqia	QBQ	100.62	36.27	2835	1953–2009
Guizhou	GZ	101.43	36.03	2237	1956–2009
Wudaoliang	WDL	93.08	35.22	4612	1956–2009
Xinghai	XH	99.98	35.58	3323	1960–2009
Tongde	TD	100.65	35.27	3289	1954–1998
Anduo	AD	91.10	32.35	4800	1965–2009
Tuotuohe	TTH	92.43	34.22	4533	1956–2009
Zaduo	ZD	95.30	32.90	4066	1956–2009
Qumalai	QML	95.78	34.13	4175	1956–2009
Yushu	YS	97.02	33.02	3681	1951–2009
Maduo	MD	98.22	34.92	4272	1953–2009
Qingshuihe	QSH	97.13	33.80	4415	1956–2009
Shiqu	SQ	98.10	32.98	4086	1960–2009
Zhongxinzhan	ZXZ	99.20	34.27	4211	1959–1997
Dari	DR	99.65	33.75	3968	1956–2009
Henan	HN	101.60	34.73	3519	1959–2009
Jiuzhi	JZ	101.48	33.43	3629	1958–2009
Maqu	MQ	102.08	34.00	3471	1967–2009
Suoxian	SX	93.78	31.88	4023	1956–2009
Dingqing	DQ	95.60	31.42	3873	1954–2009
Nangqian	NQ	96.48	32.20	3644	1956–2009
Banma	BM	100.75	32.93	3503	1960–2009
Seda	SD	100.33	32.28	3929	1961–2009
Guinan	/	*100.75*	*35.58*	*3150*	*1999–2009*
Zeku	/	*101.47*	*35.03*	*3663*	*1957–1990*
Tongren	/	*102.02*	*35.52*	*2491*	*1991–2009*
Zhiduo	/	*95.6*	*33.85*	*4179*	*1961–1990*
Guoluo	/	*100.25*	*34.47*	*3719*	*1991–2009*
Leiwuqi	/	*96.60*	*31.22*	*3810*	*1991–2009*
Shiquluoxu	/	*98.00*	*32.47*	*3399*	*1960–1981*
Aba	/	*101.7*	*32.90*	*3275*	*1954–1990*

Note. Stations in italic format are excluded in this study.

Moreover, because the autocorrelation series is not applicable for the Mann-Kendall trend test method, prewhitening (von Storch and Navarra, 1995) is required to eliminate the influence of the autocorrelation.

$$Xp_i = X_{i+1} - rX_i \tag{2}$$

where Xp_i is the observed value in the i-th year after prewhitening; r is the first-order autocorrelation coefficient of the series.

2) Change point test method

Pettitt change point test (Pettitt, 1979) is a nonparametric rank-based test used for the identification of a change point (Zhang et al., 2015). The statistical parameter K_t is given as follows:

$$K_t = \sum_{i=1}^{t}\sum_{j=t+1}^{n} sgn(X_i - X_j) = K_{t-1} + \sum_{j=1}^{n} sgn(X_t - X_j) \tag{3}$$

The probable change point T should satisfy the condition of $K_{T,n} = \mathrm{Max}_{1\le t<n}|K_t|$, and then, relationship between $K_{T,n}$ and the p value of Pettitt change point test which represents the significance level, can be expressed as follows:

$$p = 2\exp\left[-\frac{6K_{T,n}^2}{(n^3+n^2)}\right] \tag{4}$$

For a designated p value, the critical value of $K_{T,n}$ is computed first. Thereafter, each K_t is compared with this critical value to find out the significant change point in the series. In this study, the series is divided into two subsequences according to the first change point; and additional change points in these subsequences are determined if possible.

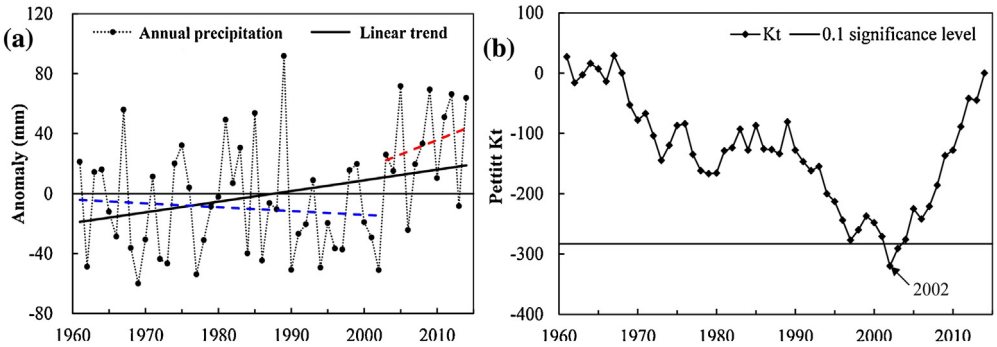

Fig. 2. Results of (a) temporal trend test and (b) change point test for the annual precipitation series in the TRH region during 1961–2014.

2.3. Spatial interpolation method

In order to compute the spatial distribution of precipitation over the TRH region, a spatial interpolation method is necessary. There are several methods available, e.g., Thiessen polygon method, inverse distance weighting (noted as IDW hereafter) method, and Kriging method. Among these methods, Thiessen polygon method, a purely geometric method, is the simplest one; however, its interpolation result is usually not satisfied. As a widely-used geometric method, the IDW method can present smoother and more accurate interpolation result than Thiessen polygon method (Goovaerts, 2000; Shi et al., 2014). Kriging method is a best-linear-unbiased-estimation method, but it is difficult to determine its variogram. With reference to the accuracy, some studies (e.g., Tabios and Salas, 1985) showed that this method can provide better results than the simpler methods (e.g. Thiessen polygon method and the IDW method), while some others (e.g., Dirks et al., 1998) showed an opposite conclusion.

Considering the simplicity and the accuracy of interpolating meteorological variables, this study selects the IDW method. A general form of the method is given as follows:

$$Z_p = \frac{\sum_{i=1}^{N} \frac{1}{D_i^{\beta}} Z_i}{\sum_{i=1}^{N} \frac{1}{D_i^{\beta}}} \tag{5}$$

where N is the number of used meteorological stations, Z_p is the value at the point of interest, Z_i is the value at the i-th given point, D_i is the distance from the i-th given point to the point of interest, and β is the power of D_i. Following common practice (Nalder and Wein, 1998; Goovaerts, 2000; Mito et al., 2011), this study adopted the value β to be 2, and the IDW method turns into the so-called inverse distance squared method.

3. Results and discussion

3.1. Temporal trend of precipitation

3.1.1. Inter-annual variation

Based on the derived annual precipitation series (1961–2014), the trend test and change point test methods were used to investigate the changing characteristics of precipitation in the TRH region. Further analyses were conducted to explain the causes.The trend in the precipitation series was tested by using the Mann-Kendall method (Fig. 2a). The mean annual precipitation (noted as MAP hereafter) was 423.0 mm in the TRH region during 1961–2014, and the annual precipitation series showed a significant increasing trend with the change rate of 7.1 mm/decade ($p < 0.1$). Moreover, the change points in the annual precipitation series were tested by using the Pettitt method. The result showed that the change point was found in 2002 at the significance level of 0.1 (Fig. 2b). However, no additional change points were found in the subsequences (i.e., 1961–2002 and 2003–2014). As a result, the annual precipitation series could be divided into two parts, namely, periods of 1961–2002 and 2003–2014, respectively. The MAP was 413.6 mm during 1961–2002, which was smaller than the long-term mean value (i.e., 423.0 mm); moreover, a decreasing trend with the change rate of −2.6 mm/decade was found in this period (the blue dash line) (Fig. 2a). In contrast, the MAP was 455.8 mm during 2003–2014, which was much larger than the long-term mean value; moreover, a significant increasing trend with the change rate of 19.3 mm/decade was found in this period (the red dash line) (Fig. 2a).

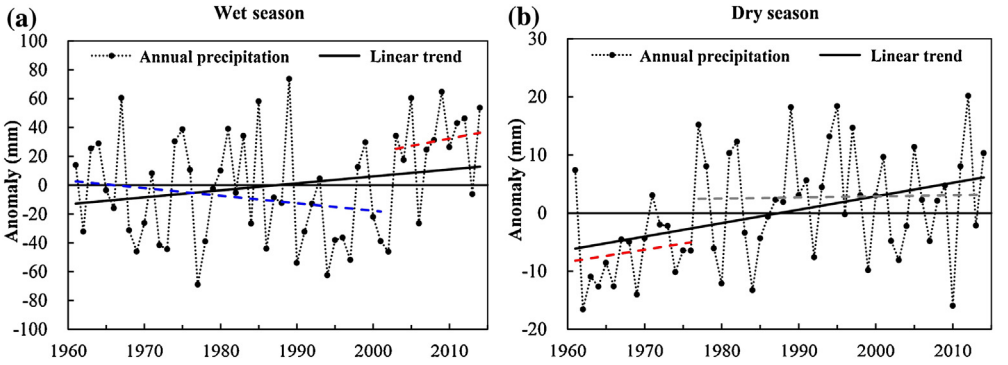

Fig. 3. Temporal trends of precipitation in the wet and dry seasons during 1961–2014.

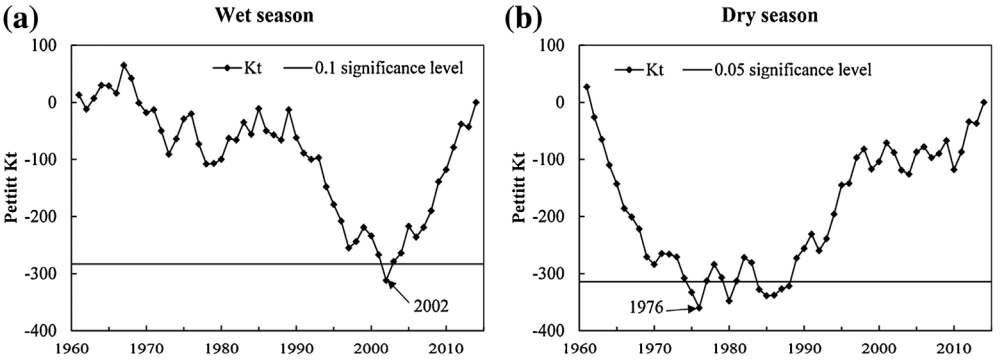

Fig. 4. Change point tests of precipitation in the wet and dry seasons during 1961–2014.

3.1.2. *Wet and dry season variations*

To further investigate the changing characteristics of precipitation in the TRH region, the trends in the wet and dry seasons were also tested by using the Mann-Kendall method. In this study, the wet season is the period from May to October, and the dry season is from November to April. The mean precipitation values were 385.8 mm in the wet season and 37.2 mm in the dry season, respectively. It indicated that the mean precipitation value of the wet season accounted for more than 90% of the annual precipitation during 1961–2014, which was ten times as large as that of the dry season. Fig. 3 shows the temporal trends of precipitation in the wet and dry seasons during 1961–2014. It is observed that precipitation of both the wet and dry seasons presented the significant increasing trends, and the change rates were 4.8 mm/decade in the wet season ($p < 0.1$) and 2.7 mm/decade in the dry season ($p < 0.01$), respectively. Compared to their mean precipitation values, the change rates were 1.26% and 7.26%, respectively, which indicated that the precipitation in the dry season had a much more pronounced increasing trend than that in the wet season.

Moreover, the change point tests were conducted for the mean precipitation series of the wet and dry seasons, respectively. For the wet season, the change point was found in 2002 at the significance level of 0.1 (Fig. 4a); in contrast, for the dry season, the change point was found in 1976 at the significance level of 0.05 (Fig. 4b); no additional change points could be found in the subsequences. As a result, the mean precipitation series of the wet and dry seasons could both be divided into two parts (Fig. 3). For the wet season, the mean precipitation was 377.0 mm with a decreasing trend (−5.2 mm/decade, the blue dash line in Fig. 3a) during 1961–2002 and 416.5 mm with an increasing trend (10.1 mm/decade, the red dash line in Fig. 3a) during 2003–2014. For the dry season, the mean precipitation was 30.5 mm with an increasing trend (2.1 mm/decade, the red dash line in Fig. 3b) during 1961–1976; while the precipitation during 1977–2014 fluctuated greatly without any trend (the gray dash line in Fig. 3b) and the mean value was 40.0 mm.

3.2. *Spatial distribution of precipitation*

Using the IDW method and the observed data recorded at the 29 meteorological stations, the spatial distribution of the MAP in the TRH region during 1961–2014 was obtained (Fig. 5a). Generally, the MAP in the TRH region showed the southeast-to-northwest decreasing trend. This is due to that the mountains on the southeastern side of this region can block the moisture from the oceans, resulting in less precipitation in the northwestern part of the TRH region (Yu et al., 2009). The famous 400-mm precipitation line in China went across the TRH region from northeast to southwest (Fig. 5a), which indicated that the TRH region lies in the border of the semi-humid and semi-arid regions. The Jiuzhi station, which locates

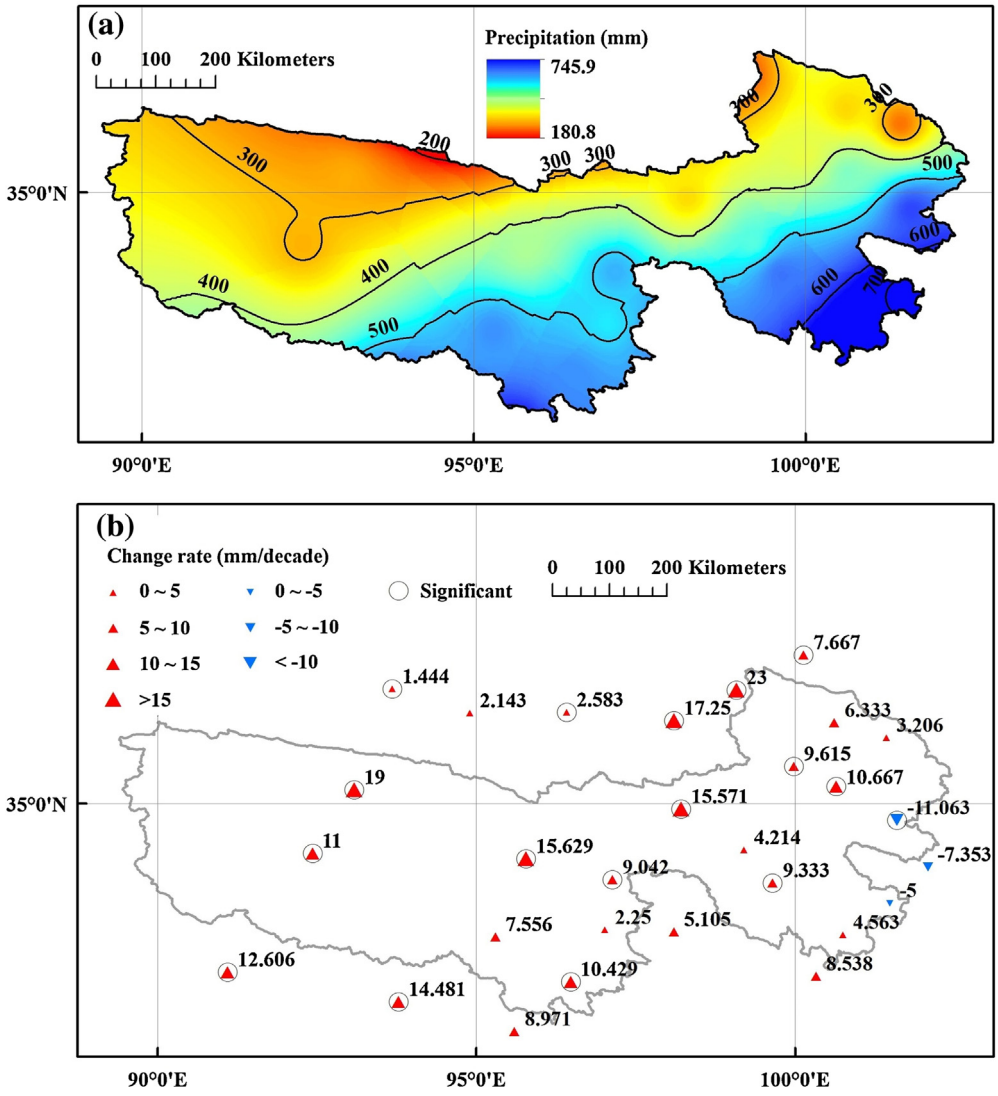

Fig. 5. Spatial distributions of (a) the mean annual precipitation and (b) the change rate of the annual precipitation in the TRH region during 1961–2014.

at the eastern edge of the TRH region, had the highest MAP of 745.9 mm; while the Xiaozhaohuo station located on the northern side of the TRH region had the lowest value of 28.3 mm, which was only about 1/26 of the highest value. However, the lowest MAP inside the TRH region was 180.8 mm.

Moreover, Fig. 5b shows the spatial distribution of the change rates of the annual precipitation recorded at the 29 meteorological stations during 1961–2014. The annual precipitation of 26 stations presented the increasing trends, and the trends in 16 stations of them were statistically significant ($p < 0.1$). Among them, the Chaka station had the highest change rate (23.0 mm/decade, $p < 0.01$), followed by the Wudaoliang station (19.0 mm/decade, $p < 0.01$) and the Dulan station (17.3 mm/decade, $p < 0.01$). However, the annual precipitation of the remaining 3 stations presented the decreasing trends, among which, only the trend in the Henan station was statistically significant (−11.1 mm/decade, $p < 0.1$). It is worth noting that these three stations were all located in the east of the TRH region. In addition, most of the stations with statistically significant trends were located in the north of the TRH region (Fig. 5b).

3.3. *Relationship between precipitation and elevation*

As mentioned above, several previous studies (e.g., Schermerhorn, 1967; Daly et al., 1994; Naoum and Tsanis, 2004; Shi, 2013) have reported the changing characteristics of precipitation along with elevation change. However, for the designated regions, different results can be obtained (e.g., Schermerhorn, 1967; Goovaerts, 2000; Chu, 2012). Through analyzing the relationship between the MAP and elevation of each meteorological station in the TRH region during 1961–2014 (see Fig. 6), these 29 stations were divided into two groups. Group I included 16 stations with the elevations lower than 3800 m, mainly

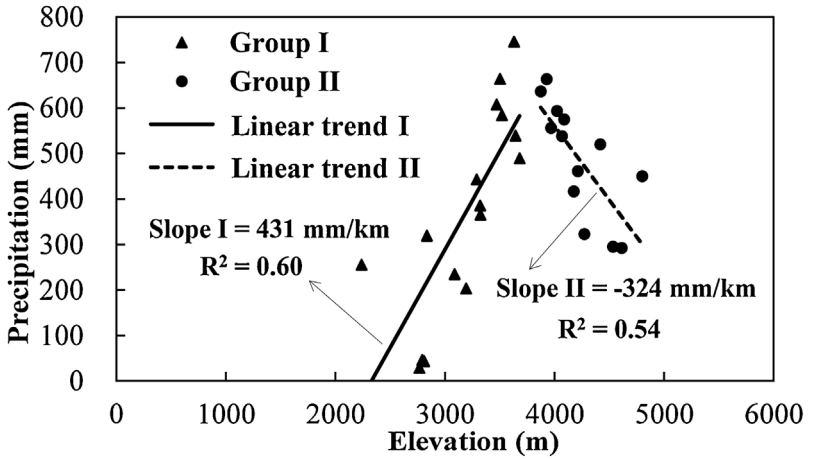

Fig. 6. Relationship between the mean annual precipitation and elevation in the TRH region during 1961–2014.

located in the northeastern part of the TRH region; while the other 13 stations with the elevations higher than 3800 m were regarded as Group II, which are mainly located in southwestern part of the TRH region. It is observed that the MAP values of the stations in Group I increased along with elevation increase, and the change rate was 431 mm/km. In contrast, for Group II, a dramatic inverse correlation was found between the MAP and elevation (i.e., −324 mm/km). As the R^2 values were not low (i.e., 0.60 for Group I and 0.54 for Group II, respectively), the relationship between precipitation and elevation in this region could approximately be expressed as follows:

$$P = \begin{cases} 0.431Z - 1005, Z < 3800m \\ -0.324Z + 1857, Z \geq 3800m \end{cases} \quad (6)$$

where P denotes the MAP (mm), and Z denotes the elevation of each meteorological station (m).

Furthermore, it is well-known that geographical location (i.e., longitude and latitude) is an important factor in influencing precipitation, as it can determine the distance between this location and the oceans, which are the main sources of moisture. Therefore, to establish better relationship between precipitation and elevation, the longitude and latitude of these 29 meteorological stations were also taken into account in this study, and the statistical equations to estimate the MAP were obtained by using the multiple regression method.

$$P = \begin{cases} 44.42X - 61.55Y + 0.193Z - 2476, Z < 3800m, R^2 = 0.96 \\ 19.79X - 88.77Y - 0.025Z + 1655, Z \geq 3800m, R^2 = 0.93 \end{cases} \quad (7)$$

where X and Y denote the longitude and latitude of each station, respectively. The R^2 values were quite high, which were 0.96 for Group I and 0.93 for Group II, respectively. Eq. (7) indicated that the MAP in the TRH region had the east-to-west and south-to-north decreasing trends, which were consistent with the analyses in previous subsection (Fig. 5a). Moreover, as the coefficient of Z was positive for Group I but negative for Group II, we concluded that the MAP increased along with increasing elevation for the stations in Group I but decreased along with increasing elevation for the stations in Group II.

Table 2 lists the comparisons of the estimated precipitation values by using Eqs. (6) and (7) and the observed mean precipitation values recorded at each station. We should be fully aware of the following two aspects. First, the results obtained from Eq. (7) were much better than those obtained from Eq. (6) in most stations, except the Gangcha, Dari and Zaduo stations. By using Eq. (7), the relative error (noted as RE hereafter) values of 25 stations (except the Xiaozhaohuo, Nuomuhong, Dulan and Maduo stations) were within ±20%, and the mean RE value of all the 29 stations was −3.7%. In contrast, by using Eq. (6), there were only 15 stations having the RE values within ±20%, and the mean RE value of all the 29 stations reached 43.4% (see Fig. 7). It is concluded that the geographical locations of the meteorological stations, which can partly reflect the impact of the monsoons, have played a great role in estimating the MAP. Second, the results of the stations in Group II were much better than those in Group I. By using Eq. (6), the mean RE values were 75.4% and 4.0% for the stations in Groups I and II, respectively; moreover, even if using Eq. (7), the mean RE values were −7.5% and 1.0%, respectively. Table 2 reveals that the large RE values mainly appeared in the stations with low elevations, where local climate may be influenced by human activities more easily than that of the stations with high elevations.

3.4. Characteristics of related meteorological variables

Generally, precipitation can be affected by a variety of related meteorological variables (Singh, 1988; Benestad, 2013; Makarieva et al., 2014). In this study, the observed data of the following related meteorological variables (i.e., air pressure,

Table 2
Comparisons of the estimated precipitation values by using Eqs. (6) and (7) and the observed mean annual precipitation values recorded at each station.

Station	Elevation (m)	Observed mean annual precipitation (mm)	Estimated by using Eq. (6) (mm)	Relative error of Eq. (6) (%)	Estimated by using Eq. (7) (mm)	Relative error of Eq. (7) (%)
GZ	2237	255.6	<0	/	243.6	−4.7
XZH	2767	28.3	187.6	563.2	<0	/
NMH	2790	46.2	197.7	328.0	102.9	122.8
GEM	2808	42.9	205.1	378.2	39.9	−7.0
QBQ	2835	318.9	216.9	−32.0	308.3	−3.3
CK	3088	234.6	325.8	38.9	257.2	9.6
DL	3191	203.1	370.4	82.4	263.2	29.6
TD	3289	442.8	412.7	−6.8	459.1	3.7
GC	3321	385.8	426.4	10.5	315.0	−18.3
XH	3323	365.7	427.3	16.8	416.5	13.9
MQ	3471	607.6	491.2	−19.2	635.8	4.6
BM	3503	663.5	504.8	−23.9	648.3	−2.3
HN	3519	584.1	511.7	−12.4	578.4	−1.0
JZ	3629	745.9	558.9	−25.1	674.4	−9.6
NQ	3644	538.8	565.4	4.9	531.1	−1.4
YS	3681	489.0	581.6	18.9	511.8	4.7
DQ	3873	635.7	602.1	−5.3	661.2	4.0
SD	3929	663.3	584.0	−12.0	676.6	2.0
DR	3968	555.9	571.5	2.8	531.9	−4.3
SX	4023	592.8	553.6	−6.6	580.1	−2.1
ZD	4066	537.7	539.5	0.3	518.8	−3.5
SQ	4086	574.2	533.1	−7.1	566.3	−1.4
QML	4175	416.3	504.3	21.1	416.2	0.0
ZXZ	4211	460.4	492.6	7.0	471.0	2.3
MD	4272	322.3	472.8	46.7	392.3	21.7
QSH	4415	519.4	426.4	−17.9	466.5	−10.2
TTH	4533	294.8	388.3	31.7	333.5	13.1
WDL	4612	291.9	362.6	24.2	255.6	−12.4
AD	4800	449.5	301.8	−32.9	466.2	3.7

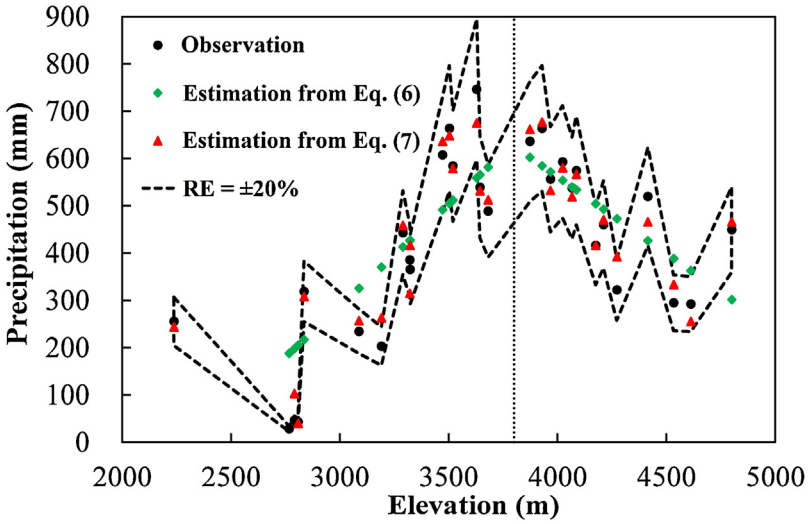

Fig. 7. Comparisons of the estimated precipitation values by using Eqs. (6) and (7) and the observed mean annual precipitation values.

air temperature, wind speed, and relative humidity) were used to investigate their impacts on precipitation (see Fig. 8). The temporal trends were tested by using the Mann-Kendall method, and the spatial distributions were obtained by using the IDW method. It is observed that air pressure and air temperature presented the statistically significant increasing trends ($p < 0.01$) while the other two variables presented the statistically significant decreasing trends (i.e., $p < 0.01$ for wind speed and $p < 0.1$ for relative humidity, respectively). These results were consistent with the conclusions of previous studies (e.g., Liang et al., 2013) to some extent, except for the small differences of the significant levels. For example, Liang et al. (2013) reported that wind speed decreased at the significant level of 0.05. Moreover, as more stations (i.e., 29 in total) were used in this study than that of Liang et al. (2013) (i.e., 12 in total), the more reliable results may be obtained. Generally, lower air pressure, higher air temperature, and faster wind may lead to higher precipitation (e.g., Back and Bretherton, 2005; Benestad, 2013; Praveen et al.,

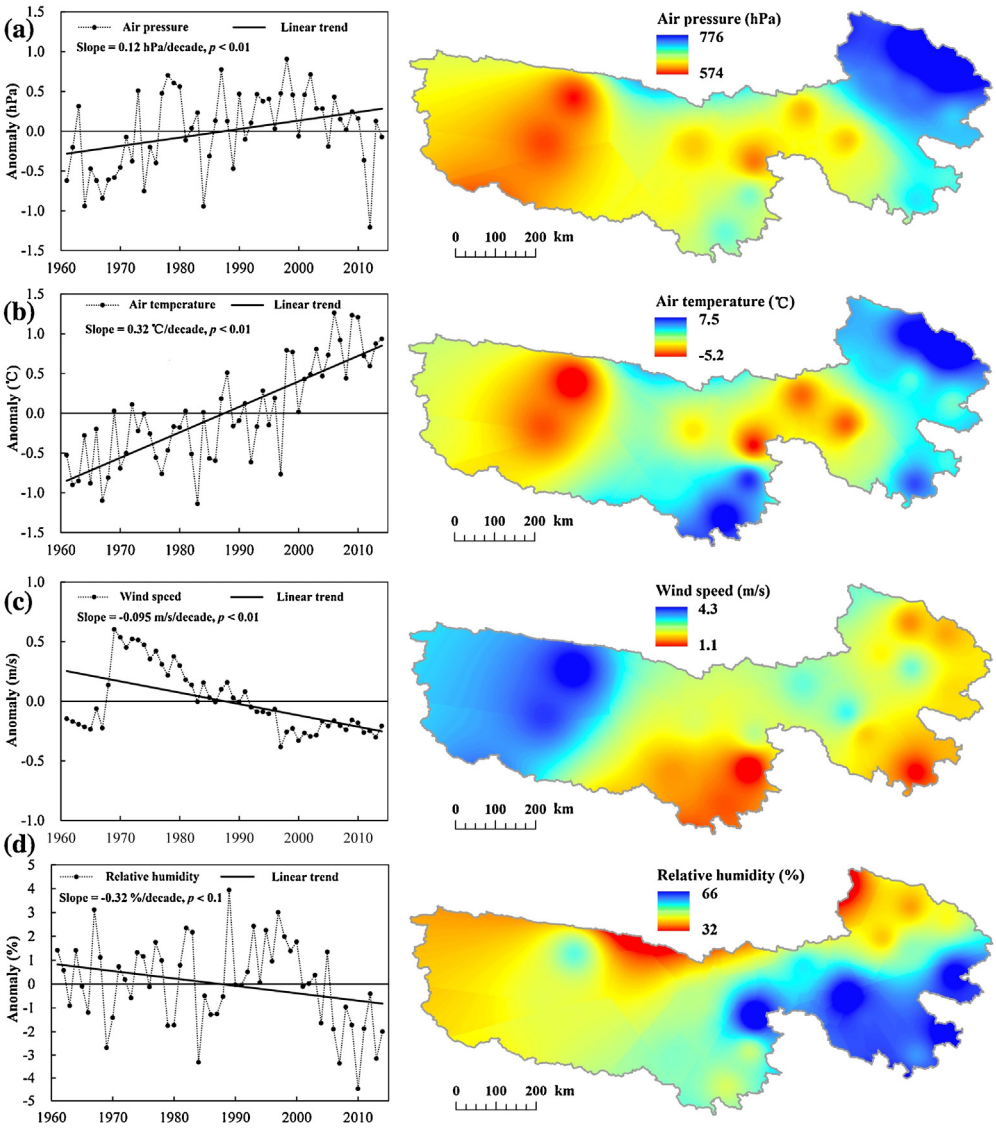

Fig. 8. Temporal trends and spatial distributions of (a) air pressure, (b) air temperature, (c) wind speed, and (d) relative humidity in the TRH region during 1961–2014.

2015). However, the present results showed that the increasing trend in air temperature (0.32 °C/decade ~ 35.5%/decade) was much more pronounced than the increasing trend in air pressure (0.12 hPa/decade ~ 0.02%/decade) and the decreasing trend in wind speed (−0.095 m/s/decade ~ −3.7%/decade). Therefore, we concluded that air temperature was the most important meteorological variable in determining precipitation. The increased air temperature may promote the transfer of water from the surface to the atmosphere, leading to the increase of the atmospheric water vapor content (You et al., 2010). In such case, the regional water circulation would be greatly speeded up, resulting in the increase of precipitation. In addition, with reference to the spatial distributions of these meteorological variables, air pressure and air temperature had the similar features, which indicated the high positive correlation between these two variables. Only the spatial distribution of relative humidity could basically match that of precipitation (see Fig. 5a).

Furthermore, large scale weather systems have played an important role in affecting the changing characteristics of precipitation. Climate in the TRH region is dominated by the Asian monsoon, which is highly complex and is influenced by large scale weather patterns (Immerzeel and Bierkens, 2010), such as the El Niño Southern Oscillation (ENSO) and the Northern Atlantic Oscillation (NAO) (Kumar et al., 1999; Yang et al., 2004). Generally, warm ENSO events can lead to the weak Indian summer monsoon (Kumar et al., 1999), and thus, less precipitation than usual. For example, warm ENSO events were recorded in the years 1969, 1972–1973 and 2002, which might partly explain the reason why the precipitation values in those years were smaller than those in the adjacent years. However, the increased air temperature over the land has helped to sustain the precipitation in the TRH region at a normal level despite warm ENSO events in recent years (e.g., years

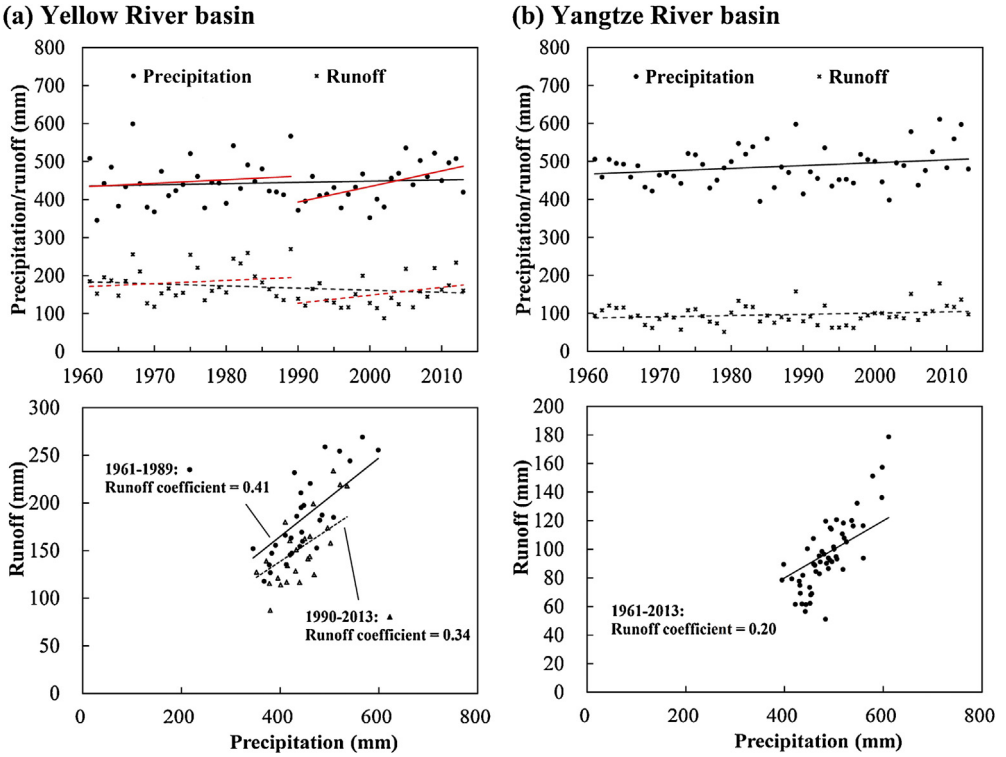

Fig. 9. Relationship between the mean annual precipitation and runoff in (a) the Yellow River basin and (b) the Yangtze River basin during 1961–2013.

1997–1998 and 2004–2005) because it may favor the enhanced land-ocean thermal gradient conducive to a strong monsoon (Kumar et al., 1999).

3.5. Possible impact on runoff

Normally, runoff should have a close correlation with precipitation in a designated region (e.g., Garbrecht et al., 2004; Luo and Wang, 2013; Shi and Wang, 2015). In this study, the annual runoff data recorded at two hydrological stations (i.e., the TNH station in the upper Yellow River and the ZMD station in the upper Yangtze River) were used to investigate the relationship between runoff and precipitation in the TRH region. Only the meteorological stations within the corresponding river basin were selected for analysis, namely, 11 meteorological stations for the Yellow River (CK, DR, GZ, HN, JZ, MD, MQ, QBQ, TD, XH, ZXZ in Fig. 1) and 8 meteorological stations for the Yangtze River (BM, QML, QSH, SD, SQ, TTH, WDL, YS in Fig. 1).

Fig. 9 shows the relationship between the MAP and runoff in these two river basins during 1961–2013. For the Yellow River basin, the R^2 value of the linear regression between these two variables was 0.50; moreover, the trend test of the annual runoff series recorded at the TNH station indicated a significant decreasing trend with the change rate of −6.26 mm/decade ($p < 0.1$). Compared to the increased precipitation (4.70 mm/decade), it is inferred that the decrease in runoff might be affected by other factors (e.g., land use changes and human activities) rather than climate change (e.g., precipitation) in this river basin. Land use changes in this region were mainly caused by grassland degradation, deforestation, desertification, and so on (Cui and Graf, 2009; Kang et al., 2010). Shao et al. (2010) showed that the land cover condition had experienced the degradation stage (from 1970s to 2004) and the ameliorative stage (from 2004 to present). Tong et al. (2014) pointed out that the wetland area in the Yellow River headwater region had decreased in general since the early 1990s; specifically, swamps and rivers, which were the dominant wetland types in the TRH region, had a continuous decreasing trend. In addition, increasing water demand due to population growth and economic expansion was regarded as another important cause of the decreased runoff. Direct water consumptions (e.g., water abstracted for irrigation, industry, and domestic uses) could account for a large proportion of the available water resources (Nakayama, 2011). Nevertheless, we can assess the impact of precipitation on runoff through calculating the increment of runoff from the increased precipitation, which could mitigate the decreasing trend in runoff. It is worth noting that the statistically significant change point was found in 1989 at the significance level of 0.05 in the annual runoff series, and therefore, the entire period could be divided into two sub-periods (i.e., 1961–1989 and 1990–2013). The sub-period 1961–1989 was regarded as the benchmark period that was less affected by human activities, and the mean annual runoff and MAP in this sub-period were 183 mm and 447 mm, respectively. Moreover, the annual runoff and precipitation increased with the change rates of 5.50 mm/decade and 7.74 mm/decade,

respectively. As the multi-year mean runoff coefficient during 1961–1989 was 0.41 (Fig. 9a), the increment of runoff due to the increased precipitation would be 3.17 (=7.74 × 0.41) mm/decade. Therefore, the increased precipitation contributed 57.6% (=3.17/5.50) to the increasing trend in runoff during 1961–1989. In contrast, the mean annual runoff and MAP in the sub-period 1990–2013 were 151 mm (82.5% of the value in the benchmark period) and 440 mm (98.4% of the value in the benchmark period), respectively, which further proved that the change in runoff might be affected not only by the change in precipitation but also by other factors (e.g., human activities). Moreover, the annual runoff and precipitation increased with the change rates of 13.51 mm/decade and 46.16 mm/decade, respectively. Regardless of other factors, the increment of runoff due to the increased precipitation would be 18.93 (=46.16 × 0.41) mm/decade. Compared to the actual change rate of runoff (13.51 mm/decade), it is inferred that other factors counteracted 28.6% (= 1-13.51/18.93) of the increased runoff due to the increased precipitation during 1990–2013. Furthermore, the multi-year mean runoff coefficient during 1990–2013 was only 0.34 (Fig. 9a).

For the Yangtze River basin, the R^2 value of the linear regression between these two variables was 0.48; moreover, the trend test of the annual runoff series recorded at the ZMD station indicated a non-significant increasing trend with the change rate of 1.91 mm/decade ($p > 0.1$), and no statistically significant change point could be found even at the significance level of 0.1. Considering the increased precipitation (5.20 mm/decade) and the multi-year mean runoff coefficient (0.20), the increment of runoff due to the increased precipitation would be 1.04 (=5.20 × 0.20) mm/decade. Therefore, in this river basin, the increased precipitation contributed 54.5% (=1.04/1.91) to the increasing trend in runoff during 1961–2013.

4. Conclusions

This study investigated the temporal trends and spatial distributions of precipitation as well as related meteorological variables, analyzed the relationship between precipitation and elevation, and discussed the possible impact of precipitation on runoff in the TRH region during 1961–2014. The main conclusions of this study can be summarized as follows.

First, the annual precipitation presented a significant increasing trend ($p < 0.1$) in this region during 1961–2014, and a more significant increasing trend ($p < 0.01$) was found in the dry season. Second, the spatial distribution of the MAP in the TRH region had the southeast-to-northwest decreasing trend, and the annual precipitation recorded at most (26 in 29) stations presented the increasing trends. Third, a low-to-high increasing trend in the MAP was found for stations with the elevations below 3800 m but an inverse correlation was found for stations with the elevations above 3800 m; moreover, statistical equations which integrated longitude, latitude and elevation were established to estimate precipitation in this region. Fourth, through analyzing the changing characteristics of related meteorological variables, we found that air temperature was the most important factor in determining precipitation in this region. Finally, the possible impact of precipitation on runoff, which could either mitigate the decreasing trend in runoff or contribute to the increasing trend in runoff in different river basins, was discussed, and we concluded that the decreased runoff in the upper Yellow River basin was mainly affected by land use changes and human activities.

This study contributed to provide a scientific basis for the changing characteristics of precipitation in mountainous regions such as the TRH region. This would be valuable for the managers to make better decisions on integrated water resources management and ecological environment assessment in the future.

Conflict of interest

The authors declare that there are no conflicts of interest.

Acknowledgements

This study was supported by the Hong Kong Scholars Program project (XJ2014059), the research project of State Key Laboratory of Hydroscience and Engineering in Tsinghua University (2014-KY-01), and the National Science & Technology Pillar Program projects in the Twelfth Five-year Plan Period (2013BAB05B05). We are also grateful to the three anonymous reviewers who offered the insightful comments leading to improvement of this paper.

References

Benestad, R.E., 2013. Association between trends in daily rainfall percentiles and the global mean temperature. J. Geophys. Res.-Atmos. 118 (19), 10802–10810.

Brassel, K.E., Reif, D., 1979. A procedure to generate Thiessen polygons. Geogr. Anal. 11, 289–303.

Burn, D.H., Elnur, M.A.H., 2002. Detection of hydrologic trends and variability. J. Hydrol. 255, 107–122.

Cao, L.G., Pan, S.M., 2014. Changes in precipitation extremes over the Three-River Headwaters region, hinterland of the Tibetan Plateau, during 1960–2012. Quat. Int. 321, 105–115.

Changnon, S.A., Demissie, M., 1996. Detection of changes in streamflow and floods resulting from climate fluctuations and land use-drainage changes. Clim. Change 32, 411–421.

Chen, Y.R., Chu, P.S., 2014. Trends in precipitation extremes and return levels in the Hawaiian Islands under a changing climate. Int. J. Climatol. 34 (15), 3913–3925.

China Meteorological Administration, 2016. Daily meteorological observation data sets of China. http://data.cma.gov.cn/data/detail/dataCode/SURF_CLI_CHN_MUL_DAY_V3.0.html.

Chu, H.J., 2012. Assessing the relationships between elevation and extreme precipitation with various durations in southern Taiwan using spatial regression models. Hydrol. Processes 26 (21), 3174–3181.
Cui, X.F., Graf, H.F., 2009. Recent land cover changes on the Tibetan Plateau: a review. Climate Change 94, 47–61.
Daly, C., Neilson, R.P., Phillips, D.L., 1994. A statistical topographic model for mapping climatological precipitation over mountainous terrain. J. Appl. Meteorol. 33, 140–158.
Dirks, K.N., Hay, J.E., Stow, C.D., Harris, D., 1998. High-resolution studies of rainfall on Norfolk Island: part II: Interpolation of rainfall data. J. Hydrol. 208 (3–4), 187–193.
Fan, J.W., Shao, Q.Q., Liu, J.Y., Wang, J.B., Harris, W., Chen, Z.Q., Zhong, H.P., Xu, X.L., Liu, R.G., 2010. Assessment of effects of climate change and grazing activity on grassland yield in the Three Rivers Headwaters Region of Qinghai-Tibet Plateau, China. Environ. Monit. Assess. 170 (1–4), 571–584.
Fan, Y.T., Chen, Y.N., Li, W.H., 2014. Increasing precipitation and baseflow in Aksu River since the 1950. Quat. Int. 336, 26–34.
Garbrecht, J., Van Liew, M., Brown, G.O., 2004. Trends in precipitation, streamflow, and evapotranspiration in the Great Plains of the United States. J. Hydrol. Eng. 9 (5), 360–367.
Goovaerts, P., 2000. Geostatistical approaches for incorporating elevation into the spatial interpolation of rainfall. J. Hydrol. 228 (1–2), 113–129.
Groisman, P.Y., Knight, R.W., Easterling, D.R., Karl, T.R., Hegerl, G.C., Razuvaev, V.N., 2005. Trends in intense precipitation in the climate record. J. Clim. 18, 1326–1350.
Intergovernmental Panel on Climate Change (IPCC), et al., 2007. Summary for policymakers, in climate change 2007: the physical science basis. In: Solomon, S. (Ed.), Contribution of Working Group I to the Fourth Assessment Report of the IPCC. Cambridge University PressCambridge, UK.
Immerzeel, W.W., Bierkens, M.F.P., 2010. Seasonal prediction of monsoon rainfall in three Asian river basins: the importance of snow cover on the Tibetan Plateau. Int. J. Climatol. 30, 1835–1842.
Immerzeel, W.W., van Beek, L.P.H., Bierkens, M.F.P., 2010. Climate change will affect the Asian water towers. Science 328, 1382–1385.
Jones, J.R., Schwartz, J.S., Ellis, K.N., Hathaway, J.M., Jawdy, C.M., 2015. Temporal variability of precipitation in the Upper Tennessee Valley. J. Hydrol.: Reg. Stud. 3, 125–138.
Kang, S.C., Xu, Y.W., You, Q.L., Flugel, W.-A., Pepin, N., Yao, T.D., 2010. Review of climate and cryospheric change in the Tibetan Plateau. Environ. Res. Lett. 5, 015101.
Kendall, M.G., 1975. Rank Correlation Measures. Charles Griffin, London.
Kumar, K., Rajagopalan, B., Cane, M.A., 1999. On the weakening relationship between the Indian monsoon and ENSO. Science 284, 2156–2159.
Liang, L.Q., Li, L.J., Liu, C.M., Cuo, L., 2013. Climate change in the Tibetan plateau three rivers source region: 1960–2009. Int. J. Climatol. 33, 2900–2916.
Liu, Q., Yang, Z.F., Cui, B.S., 2008. Spatial and temporal variability of annual precipitation during 1961–2006 in Yellow River Basin, China. J. Hydrol. 361, 330–338.
Luo, L., Wang, Z.J., 2013. Changes in hourly precipitation may explain the sharp reduction of discharge in the middle reach of the Yellow River after 2000. Front. Environ. Sci. Eng. 7 (5), 756–768.
Makarieva, A.M., Gorshkov, V.G., Sheil, D., Nobre, A.D., Bunyard, P., Li, B.L., 2014. Why does air passage over forest yield more rain? Examining the coupling between rainfall, pressure, and atmospheric moisture content. J. Hydrometeorol. 15 (1), 411–426.
Mann, H.B., 1945. Non-parametric tests against trend. Econometrica 13, 245–259.
McVicar, T.R., Van Neil, T.G., Li, L.T., Roderick, M.L., Rayner, D.P., Ricciardulli, L., Donohue, R.J., 2008. Wind speed climatology and trends for Australia, 1975–2006: capturing the stilling phenomenon and comparison with near-surface reanalysis output. Geophys. Res. Lett. 35, L20403.
Mito, Y., Ismail, M.A.M., Yamamoto, T., 2011. Multidimensional scaling and inverse distance weighting transform for image processing of hydrogeological structure in rock mass. J. Hydrol. 411 (1–2), 25–36.
Nakayama, T., 2011. Simulation of the effect of irrigation on the hydrologic cycle in the highly cultivated Yellow River Basin. Agric. Forest Meteorol. 151 (3), 314–327.
Nalder, I.A., Wein, R.W., 1998. Spatial interpolation of climatic normals: test of a new method in the Canadian boreal forest. Agric. Forest Meteorol. 92, 211–225.
Naoum, S., Tsanis, I.K., 2004. Orographic precipitation modeling with multiple linear regression. J. Hydrol. Eng. 9 (2), 79–102.
Novotny, E.V., Stefan, H.G., 2007. Stream flow in Minnesota: indicator of climate change. J. Hydrol. 334, 319–333.
Osborn, H.B., 1984. Estimating precipitation in mountainous regions. J. Hydraul. Eng. 110, 1859–1863.
Pettitt, A.N., 1979. A non-parametric approach to the change-point Problem. Appl. Stat. 28 (2), 126–135.
Praveen, V., Sandeep, S., Ajayamohan, R.S., 2015. On the relationship between mean monsoon precipitation and low pressure systems in climate model simulations. J. Clim. 28 (13), 5305–5324.
Pryor, S.C., Barthelmie, R.J., Young, D.T., Takle, E.S., Arritt, R.W., Flory, D., Gutowski Jr., W.J., Nunes, A., Roads, J., 2009. Wind speed trends over the contiguous United States. Journal of Geophysical Research 114, D14105.
Schermerhorn, V.P., 1967. Relations between topography and annual precipitation in western Oregon and Washington. Water Resour. Res. 3 (3), 707–711.
Sen, P.K., 1968. Estimates of the regression coefficient based on Kendall's tau. J. Am. Stat. Assoc. 63, 1379–1389.
Shao, Q.Q., Zhao, Z.P., Liu, J.Y., Fan, J.W., 2010. The characteristics of land cover and macroscopical ecology changes in the source region of three rivers on Qinghai-Tibet Plateau during last 30 years. Geogr. Res. 29 (8), 1139–1451 (in Chinese).
Shi, H.Y., Wang, G.Q., 2015. Impacts of climate change and hydraulic structures on runoff and sediment discharge in the middle Yellow River. Hydrol. Processes 29 (14), 3236–3246.
Shi, H.Y., Fu, X.D., Chen, J., Wang, G.Q., Li, T.J., 2014. Spatial distribution of monthly potential evaporation over mountainous regions: case of the Lhasa River basin, China. Hydrol. Sci. J. 59 (10), 1856–1871.
Shi, H.Y., 2013. Computation of spatially distributed rainfall by merging raingauge measurements, satellite observations and topographic information: a case study of the 21 July 2012 rainstorm in Beijing, China. Proceedings of the 35th IAHR World Congress, vols I and II, 530–542.
Singh, V.P., 1988. Hydrologic Systems: Watershed Modeling. Prentice Hall, New Jersey.
Tabios, G.Q., Salas, J.D., 1985. A comparative analysis of techniques for spatial interpolation of precipitation. Water Resour. Bull. 21 (3), 365–380.
Thiel, H., 1950. A rank-invariant method of linear and polynomial regression analysis, III. Proceedings of Koninalijke Nederlandse Akademie van Weinenschatpen 53, 1397–1412.
Thiessen, A.J., Alter, J.C., 1911. Precipitation averages for large areas. Mon. Weather Rev. 39, 1082–1984.
Tong, L.G., Xu, X.L., Fu, Y., Li, S., 2014. Wetland changes and their responses to climate change in the Three-River Headwaters Region of China since the 1990. Energies 7, 2515–2534.
von Storch, H., Navarra, A., 1995. Analysis of Climate Variability: Applications of Statistical Techniques. Springer-Verlag, Berlin.
Westra, S., Alexander, L.V., Zwiers, F.W., 2013. Global increasing trends in annual maximum daily precipitation. J. Clim. 26 (11), 3904–3918.
Yang, S., Lau, K.M., Yoo, S.H., Kinter, J.L., Miyakoda, K., Ho, C.H., 2004. Upstream subtropical signals preceding the Asian summer monsoon circulation. J. Clim. 17, 4213–4229.
Yi, X.S., Li, G.S., Yin, Y.Y., 2013. Spatio-temporal variation of precipitation in the Three-River Headwater Region from 1961 to 2010. J. Geog. Sci. 23 (3), 447–464.
You, Q.L., Kang, S.C., Pepin, N., Flugel, W.-A., Arturo, S.-L., Yan, Y.P., Zhang, Y.J., 2010. Climate warming and associated changes in atmospheric circulation in the eastern and central Tibetan Plateau from a homogenized dataset. Global Planet. Change 72, 11–24.
Yu, W.S., Ma, Y.M., Sun, W.Z., Wang, Y., 2009. Climatic significance of $\delta^{18}O$ records from precipitation on the western Tibetan Plateau. Chin. Sci. Bull. 54 (16), 2732–2741.
Zarch, M.A.A., Sivakumar, B., Sharma, A., 2015. Droughts in a warming climate: a global assessment of Standardized precipitation index (SPI) and Reconnaissance drought index (RDI). J. Hydrol. 526, 183–195.

Zhai, P., Zhang, X.B., Wan, H., Pan, X.H., 2005. Trends in total precipitation and frequency of daily precipitation extremes over China. J. Clim. 18, 1096–1108.
Zhang, T., Zhan, J.Y., Huang, J., Yu, R., Shi, C.C., 2013. An agent-based reasoning of impacts of regional climate changes on land use changes in the Three-River Headwaters Region of China. Adv. Meteorol., 248194.
Zhang, A.J., Zheng, C.M., Wang, S., Yao, Y.Y., 2015. Analysis of streamflow variations in the Heihe River Basin, northwest China: trends, abrupt changes, driving factors and ecological influences. J. Hydrol.: Reg. Stud. 3, 106–124.
Zhu, J.F., Zhou, Y., Wang, S.X., Wang, L.T., Wang, F.T., Liu, W.L., Guo, B., 2015. Multicriteria decision analysis for monitoring ecosystem service function of the Three-River Headwaters region of the Qinghai-Tibet Plateau, China. Environ. Monit. Assess. 187 (6), 355.